

# Variable Property Piston Effect

Howard Wagner,\* Pascal Hos,<sup>†</sup> and Yildiz Bayazitoglu<sup>‡</sup>  
Rice University, Houston, Texas 77005

**The use of the van der Waals equation of state for numerical simulation of the piston effect results in underpredicting the magnitude of the pressure wave by 38% while overpredicting the acoustic heating by 13% compared to using a real gas equation of state from the National Institute of Standards and Technology. When evaluating the piston effect at conditions typical of cryogenic storage systems, the pressure response of the fluid was observed to be tens of kilopascals. This pressure response was six orders of magnitude larger than had been reported in previous research. The extent of the acoustic heating resulted in temperature increases in the bulk fluid that was measured in tens of milliKelvins. Previous researchers reported temperature increases in microKelvins, four orders of magnitude smaller than observed in this research effort.**

## Nomenclature

$C_p$	=	specific heat at constant pressure
$C_v$	=	specific heat at constant volume
$c$	=	speed of sound
$D_{th}$	=	thermal diffusivity
$k$	=	thermal conductivity
$L$	=	characteristic length
$P$	=	pressure
$P_c$	=	critical point pressure
$T$	=	temperature
$T_{bulk}$	=	bulk fluid temperature
$T_c$	=	critical point temperature
$T_{wall}$	=	wall temperature
$t_a$	=	acoustic time, $L/c$
$t_D$	=	diffusion time, $L^2/D_{th}$
$t_H$	=	hydrodynamic time, $L^2/\nu$
$u$	=	velocity
$\alpha$	=	isothermal bulk modulus
$\beta$	=	volume expansivity
$\gamma$	=	ratio of specific heats
$\mu$	=	kinematic viscosity
$\nu$	=	dynamic viscosity
$\rho$	=	density

## Introduction

A NEW means of heat transfer known as the piston effect was identified in the late 1980s. The piston effect is where an expanding thermal boundary layer acts like a piston, which compresses the bulk fluid. The expansion of the thermal boundary layer also creates acoustic waves, which transfer energy to the bulk fluid causing a temperature rise in the bulk fluid. Previous research into the piston effect considered using only the van der Waals equation of state for conditions very close to the critical point. The research described herein compares the pressure response of oxygen using the van der Waals equation of state and a real gas equation of state provided by the National Institute of Standards and Technology (NIST).<sup>1</sup> The usual approach in estimating the time for a system to reach thermal equilibrium has been to apply the thermal diffusion equation

to the system geometry with some appropriate intermediate value of the thermodynamic properties. This approach works well when the system is far away from the critical point of the fluid. Near the critical point the experimentally measured time for thermal equilibrium indicated an equilibrium time much shorter than predicted by the diffusion equation. It was determined in the late 1980s that the effect of acoustic heating on the bulk fluid needs to be accounted for. The expanding thermal boundary layer causes a pressure wave traveling near the speed of sound in the fluid. The pressure wave contributes to an energy equation source term, which results in a nearly uniform heating of the bulk fluid. The bulk fluid temperature achieves 90% of the steady-state value in less than 5% of the time predicted by diffusion alone.

Dahl and Moldover<sup>2</sup> studied the thermal relaxation times of normal helium near the critical point. They experienced the typical slowing down of the thermal relaxation time when approaching the critical temperature from the two-phase system but experienced very fast equilibration times for the single-phase system. Nitsche and Straub<sup>3</sup> studied the variation of the specific heat at constant volume  $C_v$  near the critical point of sulfur hexafluoride ( $SF_6$ ) during the D1-Spacelab mission. The D1-Spacelab results were compared to terrestrial results and microgravity results from a previous Technologische Experimente Unter Schwerelosigkeit (TEXUS) 8 sounding rocket flight. They found that the bulk fluid temperature closely followed the boundary temperature regardless of the presence or absence of gravity. Boukari et al.<sup>4</sup> experimentally studied the thermal equilibration time for a sample of xenon at the critical density. The authors observed thermal equilibration times on the order of seconds compared to hundreds of hours predicted by pure diffusion. The fluid achieved faster thermal equilibration times when the temperature was closer to the critical temperature. Klein et al.<sup>5</sup> conducted phase transition experiments on a TEXUS sounding rocket. In the single-phase region the temperature of the fluid sample was observed to follow closely the temperature of the container wall. The rate of cooling decreased significantly in the two-phase region. The predicted thermal equilibration time was on the order of 100 h, but actual equilibration times of a few seconds were observed for the single-phase region. Garrabos et al.<sup>6</sup> and Zappoli et al.<sup>7</sup> studied the heat transport in carbon dioxide near its critical point using a TEXUS rocket. They studied the time for thermal equilibration after suddenly changing the wall temperature. The density and temperature gradients still relaxed diffusely, but the bulk fluid achieved the majority of its temperature change very quickly. The hydrodynamic time predicted for the experiment conducted by Garrabos et al.<sup>6</sup> was around 160 s. Thus, the thermal equilibration time observed is comparable to the hydrodynamic time. In two related experiments Garrabos et al.<sup>6</sup> changed the temperatures from 1 mK above to 1 mK below the critical temperature and from 1 mK below to 1 mK above the critical temperature. These experiments showed that the piston effect was still present in the two-phase region near

Received 26 December 2000; revision received 1 May 2001; accepted for publication 2 May 2001. Copyright © 2001 by the American Institute of Aeronautics and Astronautics, Inc. All rights reserved.

\*Graduate Student, Mechanical Engineering and Materials Science Department, 6100 Main St., MS 321; hwagner@rice.edu. Associate Fellow AIAA.

<sup>†</sup>Graduate Student, Mechanical Engineering and Materials Science Department, 6100 Main St., MS 321; paashaas@rice.edu.

<sup>‡</sup>H. S. Cameron Indowed Chair Professor in Mechanical Engineering, Mechanical Engineering and Materials Science Department, 6100 Main St., MS 321; bayaz@rice.edu. Member AIAA.

the critical point. Garrabos et al.<sup>8</sup> reviewed the results of a carbon dioxide critical point experiment on the TEXUS 25 sounding rocket and a sulfur hexafluoride critical point experiment on the IML-1 Spacelab mission. Both of these experiments provided evidence of the piston effect as indicated by rapid thermal equilibration of the bulk fluid and a lack of density and thermal gradients in the bulk fluid.

Guenoun et al.<sup>9</sup> conducted experiments on the TEXUS 25 sounding rocket to determine the presence of the piston effect in a sample of carbon dioxide at its critical point. Density and temperature gradients in the thermal boundary layer were unaffected by the thermal equilibration caused by the piston effect and were seen to relax diffusely. Outside of the thermal boundary layer no density or temperature gradients were present. Bonetti et al.<sup>10</sup> experimentally studied the microgravity thermal response of carbon dioxide near its critical density to varying heat inputs. They observed density gradients only within the thermal boundary layer and uniform density throughout the bulk fluid. Straub et al.<sup>11</sup> conducted experiments during the German Spacelab mission D-2 to gather microgravity data on the existence of the piston effect. They observed small temperature and density gradients in the thermal boundary layer but no gradients in the bulk fluid. The bulk fluid temperature was observed to closely follow the wall temperature.

Kassoy<sup>12</sup> conducted a theoretical investigation of the response of a confined perfect gas to a small thermal disturbance. He showed that an acoustic wave is generated in any fluid within a confined volume when the boundary temperature is suddenly changed. Boukari et al.<sup>13</sup> performed a numerical simulation of the thermal response of a layer of liquid initially at the critical point of the fluid. The authors considered both a sudden quenching of the boundaries of the one-dimensional container and a continuous increase in one of the boundary temperatures. The results were compared to data gathered from a sulfur hexafluoride (SF<sub>6</sub>) experiment conducted aboard a TEXUS sounding rocket.<sup>3</sup> When the boundary temperature was suddenly decreased from 20 mK above the critical temperature to 10 mK above the critical temperature, the bulk fluid achieved 99% of the thermal response within 5 s, significantly less time than predicted by diffusion alone. Around the same time Zappoli et al.<sup>14</sup> performed a numerical analysis of carbon dioxide and saw similar results. Onuki and Ferrell<sup>15</sup> also got similar results when they used linear hydrodynamic theory to analytically study the adiabatic heat transfer to a fluid near the critical point.

Behringer et al.<sup>16</sup> studied the thermal equilibration times for pure normal helium and mixtures of normal helium and superfluid helium. Using linearized hydrodynamic theory and Laplace transforms, they solved the Navier-Stokes and energy equations to determine the transient thermal response of the system under either constant pressure or constant volume conditions. They found that when the fluid temperature is greater than the critical temperature the thermal equilibration time for a fluid with a specific heat ratio  $\gamma \gg 1$  in a constant volume system was four times faster than for a constant pressure system. The agreement between the constant pressure and constant volume systems becomes much better when the fluid temperature is closer to the critical temperature. They also found very little difference between the equilibration times for a pure fluid and a binary fluid. The adiabatic effect was more pronounced for larger values of the specific heat ratio  $\gamma$ .

Using one-dimensional hydrodynamic theory, Zappoli<sup>17</sup> and Djennaoui et al.<sup>18</sup> performed an asymptotic solution of the one-dimensional Navier-Stokes equation for a van der Waals fluid near the critical point. Their predicted thermal equilibration time agrees with the predictions of Onuki and Ferrell.<sup>15</sup> Later Zappoli et al.<sup>19</sup> extended their previous one-dimensional hydrodynamic equations to include two-dimensional unsteady heat-transfer effects. Their efforts demonstrated that the piston effect was still present in a normal Earth gravity condition and results in fast thermal equilibration of the bulk fluid prior to the onset of buoyancy-driven convection. The density gradient remaining after the thermal equilibration is the driving mechanism for the onset of convection.

Because the piston effect requires knowledge of the fluid properties near the critical point, an accurate model of the equation of

state is needed. Typical analytical forms of the equation of state predict finite values of the specific heats  $C_p$  and  $C_v$ , the thermal conductivity, and the speed of sound at the critical point. It is well established by experimental results that the specific heats and the thermal conductivity diverge to infinity as the critical point is approached. The use of an empirical equation of state is required to adequately model the change in the fluid properties near the critical point. Hendricks et al.<sup>20</sup> developed a computer program to provide the thermophysical properties of 10 different cryogenic fluids. The program did not attempt to model the anomalous behavior near the critical point and therefore could not be utilized for this research effort. Emanuel<sup>21</sup> applied critical point theory to predict the thermodynamic properties of a real fluid near the critical point. The theory is applicable to any fluid and accurately predicts the divergence of the properties of interest at the critical point. The use of critical point theory needs further investigation and is beyond the scope of this research. Nwobi et al.<sup>22</sup> used molecular dynamics theory to predict the thermodynamic properties of supercritical oxygen. The approach accurately predicts the divergence of certain important properties near the critical point but is much too computer time intensive to be of any practical use in numerical simulations.

The thermodynamic properties utilized in this research effort were calculated using a computer program originally created by the NIST<sup>1</sup> in 1980 for the NASA Johnson Space Center. The program reproduces the values from the published NIST tables for 15 cryogenic fluids. The program accurately reproduces the divergence of the fluid properties at the critical point. The output from the program was compared to the published tables from NIST with very close correlation, often within 1% of the tabulated values except near the critical point where the maximum error is estimated to be about 10%. Readers interested in the details of the equations provided by NIST are referred to the report from NIST.<sup>1</sup>

The research described in the literature review focused on the fast thermal equilibration of a fluid near the critical point. All of the previous researchers used only the van der Waals equation of state to evaluate the density of the fluid. The research presented here focuses on the pressure and temperature changes in a fluid near the critical point and compares results from the van der Waals equation of state to the results obtained using the NIST equation of state. The temperatures investigated in this research effort also include bulk fluid temperatures significantly below the critical temperature, which were not investigated previously. All of the previous research looked at conditions within a few mK of the critical temperature. The physics that result in large pressure changes caused by changes in the thermal boundary-layer thickness are described in the following section.

## Theory

A theoretical basis for predicting the pressure sensitivity of a fluid near the critical point can be developed by examining the equations of motion and heat transfer. From the fundamental equations the significant fluid properties can be identified, and their contribution to the fast thermal equilibration and extreme pressure sensitivity of a fluid near the critical point can be explained. The conservation equations for an unsteady one-dimensional system are given by Eqs. (1–3) for mass, momentum, and energy, respectively:

$$\frac{\partial \rho}{\partial t} + \frac{\partial}{\partial x}(\rho u) = 0 \quad (1)$$

$$\frac{\partial \rho u}{\partial t} + \frac{\partial \rho u^2}{\partial x} = -\frac{\partial P}{\partial x} + \frac{\partial}{\partial x} \left( \frac{4}{3} \mu \frac{\partial u}{\partial x} \right) \quad (2)$$

$$\begin{aligned} \frac{\partial}{\partial t}(\rho T) + \frac{\partial}{\partial x} \left( \rho u T - \frac{k}{C_v} \frac{\partial T}{\partial x} \right) = & -\frac{T}{C_v} \left( \frac{\partial P}{\partial T} \right)_\rho \left( \frac{\partial u}{\partial x} \right) \\ & + \frac{k}{C_v^2} \left( \frac{\partial T}{\partial x} \frac{\partial C_v}{\partial x} \right) \end{aligned} \quad (3)$$

Boundary conditions:

$$\frac{\partial P}{\partial x} = 0 \quad \text{at} \quad x = 0, L \quad (4)$$

$$u = 0 \quad \text{at} \quad x = 0, L \quad (5)$$

$$T = T_c + 1 \text{ K} \quad \text{at} \quad x = 0 \quad (6)$$

$$T = T_{\text{bulk}} \quad \text{at} \quad x = L \quad (7)$$

Initial conditions:

$$P = P_c \quad (8)$$

$$T = T_{\text{bulk}} \quad (9)$$

$$U = 0 \quad (10)$$

For most fluids the pressure gradient dominates the momentum equation source term because the viscosity is very small. This is valid for cryogenic fluids regardless of the proximity to the critical point. Gravity effects are not included in either the momentum or energy equations. The acoustic heating caused by the piston effect is very small, and the presence of gravity would induce convective heat transfer, which would mask the effects from the acoustic heating. This form of the energy equation for a compressible fluid is a slight modification of the form given by Arpaci and Larsen.<sup>23</sup> The difference is that the specific heat was brought inside of the derivative for the thermal conductivity. This results in creating a source term involving the derivative of the specific heat. A dimensional analysis was performed on the entire energy equation to determine which portions of the source term are of significance. The viscous heating contribution was determined to be 10 orders of magnitude smaller than the acoustic heating term and can be neglected. The contribution from the kinetic heating and diffusion terms were also neglected with respect to the acoustic heating term. This results in keeping only the acoustic heating and variable specific heat contributions to the source term. All of the source terms were included in the computer code. The computer code was implemented such that the user could enable or disable the individual contributions to the energy equation source term. Numerous runs were conducted to verify that neglecting the diffusion, viscous, and kinetic heating terms did not impact the solution. Reflection boundary conditions are applied at both the left and right boundaries, which gives zero pressure gradient and zero velocity at each boundary. If the bulk fluid is initialized at temperatures very close to the critical temperature, then the pressure boundary condition at the right plate has to be change from a reflection condition to an outflow boundary condition.<sup>24</sup> The conditions encountered during this research effort did not require this change in the pressure boundary condition. The right boundary is maintained at the bulk fluid temperature while the left boundary is set to 1 K above the critical temperature. The fluid is initially at rest with the pressure at the critical pressure and the fluid temperature at  $T_{\text{bulk}}$ .

Looking at the energy equation (3), some additional observations can be made. As the fluid approaches the critical point,  $C_v$  increases greatly, and the effect of the right-hand side can be neglected. Thus the effect of acoustic heating is important only outside of the thermal boundary layer. On the left-hand side of the equation, the thermal conductivity/specific heat ratio diverges to infinity, and the thermal gradient term dominates the time dependence of the temperature. From the energy equation source term it can be seen that heating in the bulk fluid is caused by the fluid motion. The pressure derivative acts as an amplification factor and is evaluated based upon the particular equation of state being used. From the real gas equation of state, this pressure derivative is given as

$$\left( \frac{\partial P}{\partial T} \right)_\rho = -\alpha\beta \quad (11)$$

where  $\alpha$  is the isothermal bulk modulus

$$\alpha = -\rho \left( \frac{\partial P}{\partial \rho} \right)_T \quad (12)$$

and  $\beta$  is the volume expansivity

$$\beta = \frac{(1/\rho)(\partial P/\partial T)_\rho}{(\partial P/\partial \rho)_T} \quad (13)$$

For a van der Waals fluid  $P = \rho RT/(1 - \rho b) - a\rho^2$ , the pressure derivative reduces to

$$\left( \frac{\partial P}{\partial T} \right)_\rho = \frac{\rho R}{1 - \rho b} \quad (14)$$

where the isothermal bulk modulus is

$$\alpha = -\rho \left( \frac{\partial P}{\partial \rho} \right)_T = - \left[ \frac{b\rho^2 RT}{(1 - b\rho)^2} + \frac{\rho RT}{(1 - b\rho)} - 2a\rho^2 \right] \quad (15)$$

and the volume expansivity is

$$\begin{aligned} \beta &= \frac{(1/\rho)(\partial P/\partial T)_\rho}{(\partial P/\partial \rho)_T} \\ &= \frac{\rho R/(1 - \rho b)}{b\rho^2 RT/(1 - b\rho)^2 + \rho RT/(1 - b\rho) - 2a\rho^2} \end{aligned} \quad (16)$$

The thermal diffusivity for a constant-pressure process is given by  $D_{\text{th}} = k/\rho C_p$ . When approaching the critical point,  $C_p$  diverges about twice as fast as the thermal conductivity, and therefore the thermal diffusivity goes to zero. Thus extremely long thermal equilibration times are predicted. This leads to the common observation of slowing down of thermal equilibration when approaching the critical point. This is seen to hold only for a constant pressure process. The thermal diffusivity for a constant volume process is given by  $D_{\text{th}} = k/\rho C_v$ . In this case the thermal conductivity diverges faster than  $C_v$ , and the thermal diffusivity goes to infinity. Therefore the thermal equilibration time for a constant volume process will approach zero. The thermal equilibration actually speeds up when approaching the critical point.

Three different timescales are identified in this problem: 1) the acoustic time  $t_a = L/c$ , 2) the hydrodynamic time  $t_H = L^2/\nu$ , and 3) the diffusion time  $t_D = L^2/D_{\text{th}}$ . The acoustic time is the time required for the pressure wave to travel the length of the container. The hydrodynamic time is the time required for the fluid motion to come back to rest via viscous dissipation. The diffusion time is the time for a temperature change to be transmitted the length of the container by pure diffusion. The hydrodynamic time is slightly greater than the acoustic time, both of which are significantly less than the diffusion time. Acoustic waves are created by the changing thermal boundary-layer thickness during the heating and cooling of the heat-transfer surface and dissipate shortly after a stable boundary temperature is achieved. These acoustic waves are the mechanism by which heat is transferred from the heat-transfer surface to the bulk fluid. This process is referred to as the piston effect. Kassoy<sup>12</sup> showed that the strength of the acoustic wave is dependent on the magnitude of the temperature change and how rapidly the fluid properties vary with temperature. Because the fluid properties show the greatest sensitivity at the critical point, this suggests that the acoustic waves will be strongest when near the critical point of the fluid.

## Analysis

The thermophysical properties involved are the density, thermal conductivity, constant volume specific heat, isothermal compressibility (the inverse of the isothermal bulk modulus), and the volume expansivity. The properties of oxygen will be examined to determine what differences in behavior from the two equations of state are noticeable. The most important properties for the piston effect were determined to be the thermal conductivity, the volume expansivity, and the isothermal compressibility. The thermal conductivity and the volume expansivity determine the thickness of the thermal boundary layer. Experimental and numerical analyses have shown that the thermal boundary layer can be considered to be a piston

compressing or expanding the bulk fluid. The isothermal compressibility determines the pressure response of the bulk fluid caused by a change in volume of the thermal boundary layer.

A solution algorithm was desired that could handle the extreme compressibility expected near the critical point. The semi-implicit method for pressure linked equations algorithm developed by Patankar<sup>25</sup> was selected because it avoids the problems that could be encountered with most solution algorithms that employ the speed of sound as a scaling factor to normalize the fluid velocities. The fluid velocities encountered in this research are very small, and scaling with the speed of sound would increase the stiffness of the solution matrix. Because the algorithm treats only the time step explicitly and all other parameters implicitly, it allows for a wide range of time step and grid sizes while providing a stable solution.

The situation being evaluated is the pressure and temperature increase in oxygen at the critical pressure of 5043 kPa contained between two infinite parallel plates. The plates were fixed with a separation distance of 2.5 mm. The bulk fluid was initialized to a temperature ranging from 0.50 to 1.00 times the critical temperature of 154.58 K in increments of 0.05 times the critical temperature, and then one plate would undergo a step change to 1 K above the critical temperature. The simulations employed a time step of half the acoustic time period  $t_a/2$  and ran for a total of five acoustic time periods  $5t_a$ . The acoustic time period was adjusted for each run based on the speed of sound in the bulk fluid. The peak pressure showed a 5% change when the number of nodes was increased from 5000 to 10,000. When the number of nodes was increased from 10,000 to 15,000, the peak pressure changed by less than 1%. Based on this grid sensitivity analysis, it was determined that 10,000 nodes would provide an acceptable accuracy.

Three sets of conditions were studied in this research effort. First, the van der Waals equation of state was used to evaluate the density, volume expansivity, and isothermal compressibility. The thermal conductivity, specific heat, and viscosity were held constant at the initial conditions of the bulk fluid, using values provided by the NIST.<sup>1</sup> This is the procedure used by the previous researchers who used only the van der Waals equation of state. Repeating their procedures gives a direct comparison to the prior research efforts. Next, the NIST equation of state was used to evaluate the density, volume expansivity, and isothermal compressibility. The thermal conductivity, specific heat, and viscosity were again held constant at the initial conditions of the bulk fluid, using values provided by the NIST. This provides a direct assessment of how the equation of state affects the pressure and temperature response of a fluid. Finally, all fluid properties were evaluated as a function of pressure and temperature, based on equations provided by the NIST. This final condition evaluates the effect of variable fluid properties on the pressure and temperature response. The fluid properties were evaluated at each of the 10,000 nodes. Predictions of the pressure and temperature changes caused by a thermal disturbance were made by evaluating the thermophysical properties, and then the predictions were compared to the numerical results.

The variation of the density and the pressure derivative ( $\partial P/\partial T$ )<sub>p</sub> with temperature based on the use of the van der Waals and NIST equations of state are compared in Fig. 1. The pressure is held constant at the critical pressure of oxygen, 5043 kPa. The density prediction from the van der Waals equation of state underpredicts the actual density by approximately 30% over most of the temperature range. The van der Waals equation of state became unstable for temperatures below 100 K. The density is solved by iterating on the van der Waals equation of state. This iterative process fails to converge to a stable solution below 100 K. This is expected because the van der Waals equation of state is a modification of the ideal gas law and does not provide a good density prediction for the sub-cooled liquid state. The van der Waals equation provides a good estimate for the saturated liquid state, but the error increases as the fluid conditions get farther away from the saturation condition. In the compressed gas region, above 156 K the correlation is much closer. The 30% reduction in density would require a corresponding increase in the velocity in order to satisfy the conservation of continuity. Therefore it is expected that the velocity of the bulk fluid

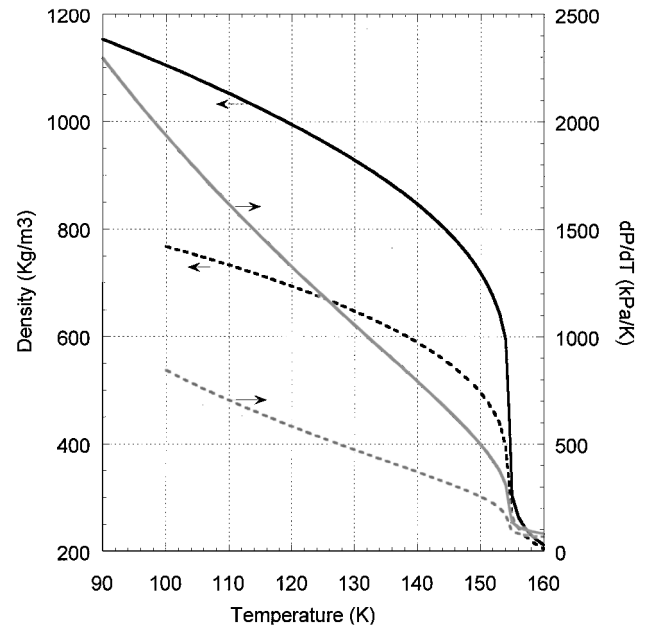


Fig. 1 Variation of the density and the pressure derivative with temperature at 5043 kPa: —, values from the NIST equation of state; and ---, values using the van der Waals equation of state.

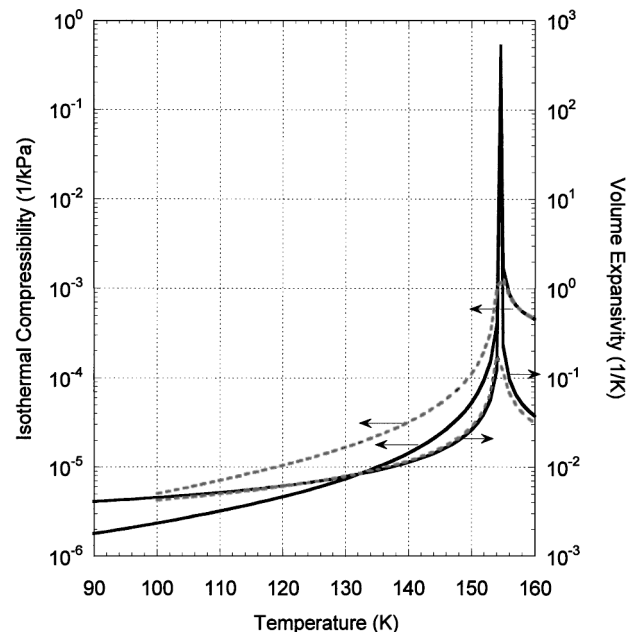


Fig. 2 Variation of the isothermal compressibility and the volume expansivity with temperature at 5043 kPa: —, values from the NIST equation of state; and ---, values using the van der Waals equation of state. The isothermal compressibility is shown multiplied by  $-1$  for plotting purposes.

after the passage of the pressure wave will exhibit higher velocities when using the van der Waals equation of state. The van der Waals equation of state overpredicts the pressure derivative by a factor of two. The pressure derivative is used in the energy equation source term, and therefore it is expected to observe less heating in the bulk fluid when using the van der Waals equation of state compared to the NIST equation of state.

The pressure derivative can be decomposed into the isothermal compressibility and the volume expansivity. The variation of the isothermal compressibility and the volume expansivity with temperature based on the use of the van der Waals and NIST equations of state are compared in Fig. 2. The isothermal compressibility

is shown multiplied by  $-1$  to simplify the plot. The pressure is again held constant at the critical pressure of oxygen, 5043 kPa. The volume expansivity determines how much the thermal penetration region will expand as a result of the temperature increase at the boundary. The van der Waals equation of state does a fairly good job of reproducing the volume expansivity. It even predicts the divergence at the critical temperature. The isothermal compressibility determines the pressure response of the bulk fluid caused by the change in volume of the thermal boundary layer. The van der Waals equation of state reproduces the divergence in the isothermal compressibility at the critical point. Over the majority of the subcooled liquid region, the van der Waals equation of state overpredicts the compressibility by a factor of two. This shows that the error in the pressure derivative caused by using the van der Waals equation of state is entirely a result of the error in the isothermal compressibility. A larger absolute value of the isothermal compressibility indicates a greater compressibility of the fluid. A larger volume change would therefore occur for a small pressure change when near the critical point. The inverse would also hold true, for a large volume change the pressure would change only a small amount when near the critical point. If the fluid is much colder than the critical temperature, then the fluid will respond as an incompressible liquid. Therefore the compressibility effects will be isolated to the thermal penetration region. The van der Waals equation of state will underpredict the pressure response of the bulk liquid by a factor of two. This effect had not been encountered in prior research because all of the previous numerical investigations of the piston effect were evaluated using only the van der Waals equation of state at conditions very close to the critical point.

All of the remaining fluid properties are evaluated from the NIST computer program.<sup>1</sup> The variation of the thermal conductivity and the specific heat at constant volume with temperature are shown in Fig. 3. The pressure is again held constant at the critical pressure of oxygen, 5043 kPa. The thermal conductivity of the liquid oxygen decreases by a factor of four as the temperature increases toward the critical temperature. There is a large divergence at the critical point, and then the thermal conductivity continues to decrease as the oxygen temperature continues to increase. The specific heat at constant volume shows only a slight variation in the liquid region. There is a large divergence at the critical temperature, and then the value continues to decrease as the temperature is increased. The van der Waals numerical analyses and the NIST numerical analyses using fixed fluid properties use the same thermal conductivity so that

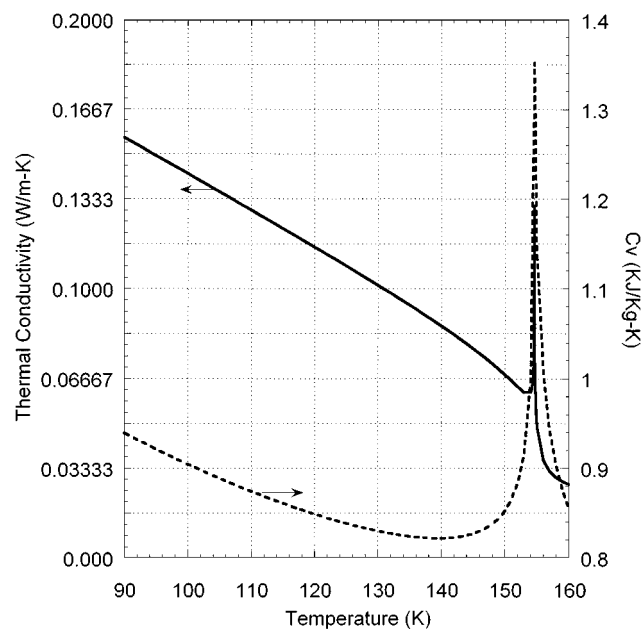


**Fig. 3** Variation of the thermal conductivity and the specific heat at constant volume with temperature at 5043 kPa. Both functions are from values given by the NIST.

**Table 1** Speed of sound and acoustic times used for the numerical simulations

Temperature, K	Reduced temperature, $T/T_c$	Speed of sound, m/s	Acoustic time, $\mu s$
154.581	1.00	154.15	16.22
146.85	0.95	388.19	6.44
139.12	0.90	492.08	5.08
131.39	0.85	576.40	4.34
123.66	0.80	650.98	3.84
115.94	0.75	719.60	3.47
108.21	0.70	784.49	3.19
100.48	0.65	846.82	2.95
92.75	0.60	907.54	2.76
85.02	0.55	967.37	2.58
77.29	0.50	1026.72	2.44

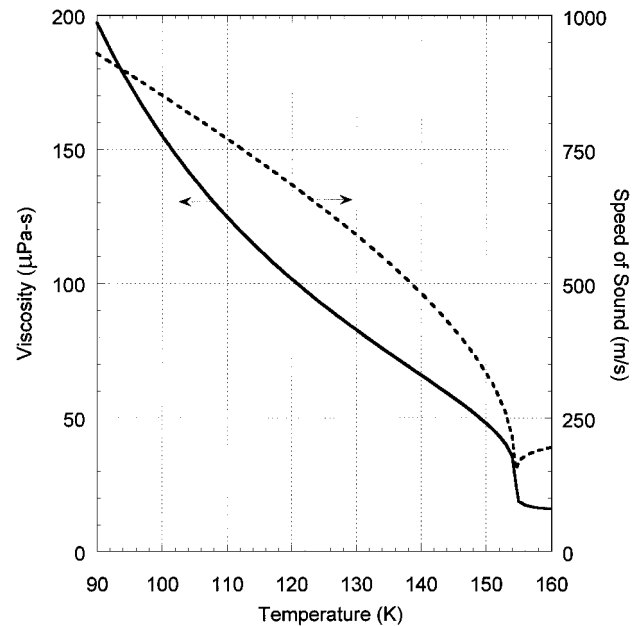


**Fig. 4** Variation of the viscosity and the speed of sound with temperature at 5043 kPa. Both functions are from values given by the NIST.

the thickness of the penetration depth region will be the same. The NIST numerical analyses using variable fluid properties will result in a higher thermal conductivity in the penetration depth region as a result of the divergence of the thermal conductivity at the critical point. This will result in a thinner penetration depth compared to using fixed fluid properties. The thinner penetration depth will result in a lower pressure increase compared to the analyses using fixed fluid properties.

The variation of the viscosity and the speed of sound with temperature are shown in Fig. 4. The pressure is again held constant at the critical pressure of oxygen, 5043 kPa. The viscosity of oxygen decreases by a factor of four as the oxygen is heated up. There is a sharp decrease in the viscosity at the critical temperature and then a gradual decrease as the gaseous oxygen is heated further. The speed of sound decreases as the fluid is heated to the critical temperature and then stabilizes at approximately 200 m/s for the gas phase. For each numerical simulation the speed of sound was evaluated based on the initial temperature of the bulk fluid and was held constant for each run. The values used in the numerical analyses are shown in Table 1.

The following numerical results were all evaluated using a reduced temperature of the bulk fluid of 0.85. The reduced temperature is defined as the fluid temperature divided by the critical temperature. The velocity and pressure profile after half an acoustic time period are presented in Figs. 5 and 6, respectively. The peak velocity from the van der Waals run is 43% higher than the velocity from the NIST run using fixed fluid properties. This increase in the

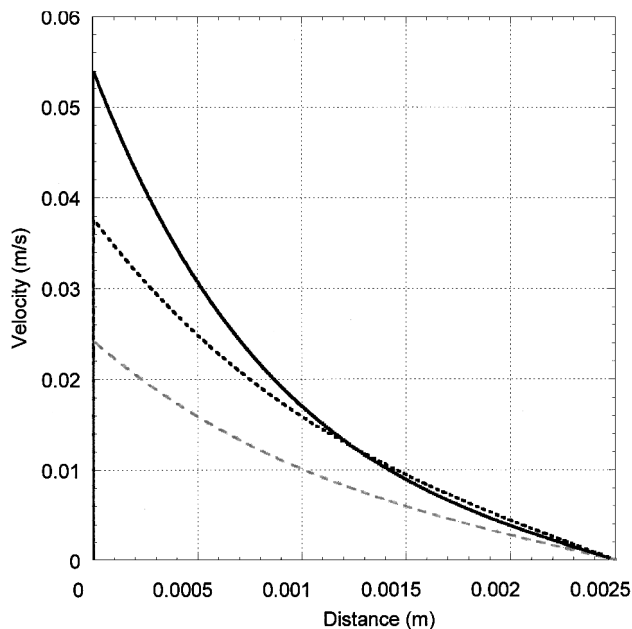


Fig. 5 Velocity profiles after half an acoustic time period: —, data from the van der Waals equation of state; ···, data using the NIST equation of state with fixed fluid properties; and ---, data using the NIST equation of state with variable fluid properties.

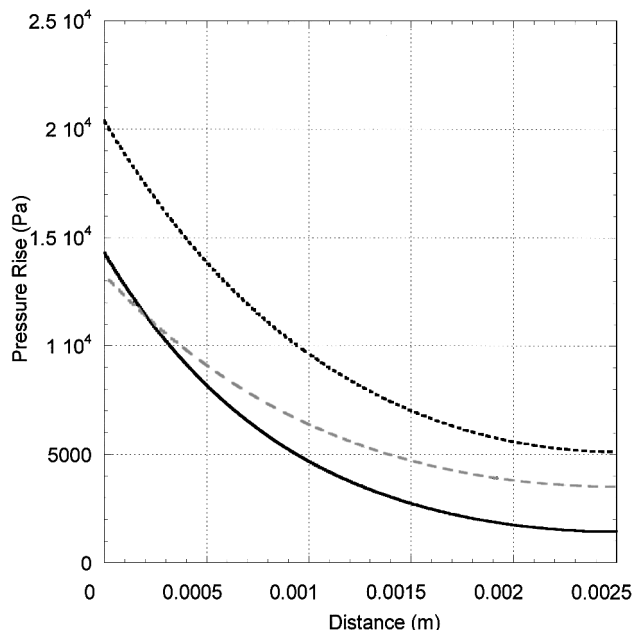


Fig. 6 Pressure increase after half an acoustic time period: —, data from the van der Waals equation of state; ···, data using the NIST equation of state with fixed fluid properties; and ---, data using the NIST equation of state with variable fluid properties.

velocity was predicted based on the lower density given by the van der Waals equation of state. The peak pressure for the van der Waals run is seen to also be 30% lower compared to the NIST run with fixed fluid properties. The peak pressure for the van der Waals run using fixed fluid properties is seen to be 8% higher than the NIST run using variable fluid properties. The van der Waals equation of state overpredicts the peak velocity by 123% compared to the NIST run using variable fluid properties. From the preceding discussion of the thermal conductivities, it was predicted that the pressure rise would be larger when using fixed fluid properties.

The pressure rise and temperature rise was nearly uniform after five acoustic time periods. The total pressure rise from the van der

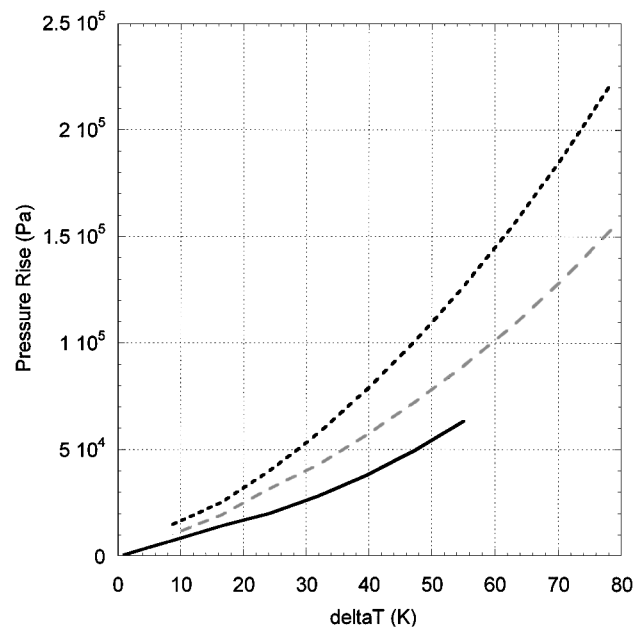


Fig. 7 Pressure increase after five acoustic time periods: —, data from the van der Waals equation of state; ···, data using the NIST equation of state with fixed fluid properties; and ---, data using the NIST equation of state with variable fluid properties.

Waals run was 20 kPa while the pressure rise from the NIST run using fixed fluid properties was 40 kPa. The total pressure rise from the van der Waals run is half of the pressure rise from the NIST run using fixed fluid properties. This is in agreement with the factor of two underprediction of the isothermal compressibility by the van der Waals equation of state. The total pressure rise from the NIST run using variable fluid properties was 32 kPa. The van der Waals run underpredicted the pressure rise by 38% compared to the NIST run using variable fluid properties. The total temperature rise in the bulk fluid from the van der Waals run was 21 mK while the temperature rise from the NIST run using fixed fluid properties was 23 mK. The factor of two decrease in the isothermal compressibility offsets the 44% lower velocity to result in underpredicting the bulk heating from the van der Waals run by 9% compared to the NIST run with fixed fluid properties. The temperature rise of the bulk fluid was 18 mK for the NIST run using variable fluid properties. The van der Waals run with fixed fluid properties overpredicts the temperature rise by 17% compared to the NIST run with variable fluid properties.

The resulting pressure rise after five acoustic time periods is shown in Fig. 7 as a function of the amount of subcooling of the bulk fluid. The temperature difference is defined as the difference between the heater temperature and the bulk fluid temperature. For all runs the heater temperature was set at 1 K above the critical temperature. It is seen that the van der Waals equation of state consistently underpredicts the magnitude of the pressure rise by approximately 38% while using the NIST equation of state with fixed fluid properties consistently overpredicts the pressure rise by approximately 25%. Pressure increases of multiple kPa are achievable with subcooling as low as 20 K below the critical temperature. A supercritical liquid oxygen tank loaded with normal boiling point oxygen and then pressurized to the critical pressure will have a bulk fluid temperature of 90 K or 64 K of subcooling. A pressure increase greater than 10 kPa could result if a submerged heater surface is then heated to the critical temperature. Zappoli et al.<sup>14</sup> reported a pressure rise of 0.01 Pa at a 1 K subcooled condition. The pressure rise observed in this research effort is six orders of magnitude larger than previously reported values.

The temperature increase in the bulk fluid after five acoustic time periods is shown in Fig. 8 as a function of the amount of subcooling of the bulk fluid. It is seen that both the van der Waals runs and the NIST runs using fixed fluid properties overpredict the extent of the acoustic heating. The van der Waals equation of state with

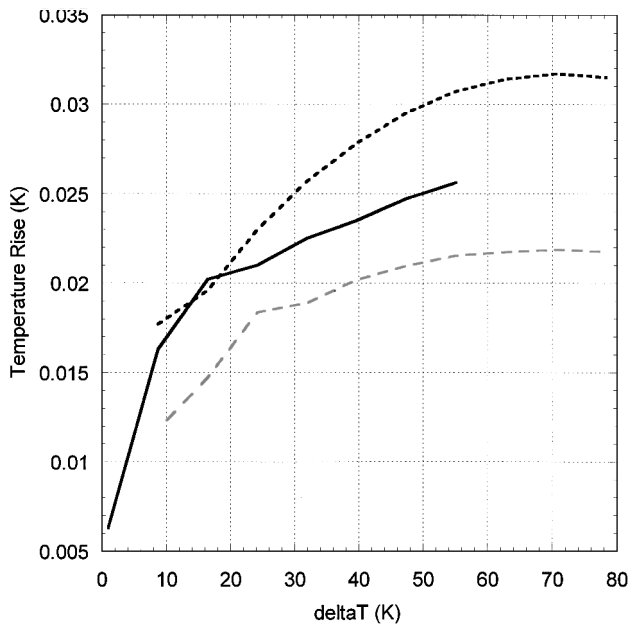


Fig. 8 Bulk fluid temperature increase after five acoustic time periods: —, data from the van der Waals equation of state; ····, data using the NIST equation of state with fixed fluid properties; and ---, data using the NIST equation of state with variable fluid properties.

fixed fluid properties overpredicts the amount of acoustic heating by approximately 13%. Using fixed fluid properties with the NIST equation of state overpredicts the acoustic heating by approximately 40%. At 64 K of subcooling the temperature increase is over 20 mK compared to 2  $\mu$ K at 1 K of subcooling.<sup>14</sup> The temperature rise observed during this research effort is four orders of magnitude larger than any temperature rise reported in the literature.

### Conclusions

The use of the van der Waals equation of state for numerical simulation of the piston effect results in underpredicting the magnitude of the pressure wave by approximately 38% while overpredicting the acoustic heating by approximately 13% compared to using all fluid properties from the NIST.<sup>1</sup> When evaluating the piston effect at conditions typical of cryogenic storage systems, the pressure response of the fluid was observed to be six orders of magnitude larger than had been previously reported. The extent of the acoustic heating resulted in temperature increases in the bulk fluid that were four orders of magnitude larger.

### References

- <sup>1</sup>McCarty, R. D., "Interactive Fortran IV Computer Programs for the Thermodynamic and Transport Properties of Selected Cryogenics (Fluids Pack)," National Bureau of Standards, TN 1025, U.S. Dept. of Commerce, Washington, DC, Oct. 1980.
- <sup>2</sup>Dahl, D., and Moldover, M. R., "Thermal Relaxation Near the Critical Point," *Physical Review A: General Physics*, Vol. 6, Nov. 1972, pp. 1915–1920.
- <sup>3</sup>Nitsche, K., and Straub, J., "The Critical 'Hump' of  $C_v$  Under Microgravity Results From the D1-Spacelab Experiment 'Warmekapazität'," *Proceedings of the Sixth European Symposium on Material Sciences Under Microgravity Conditions*, Vol. SP-256, European Space Agency, Noordwijk, The Netherlands, 1986, pp. 109–116.
- <sup>4</sup>Boukari, H., Briggs, M. E., Shaumeyer, J. N., and Gammon, R. W., "Critical Speeding Up Observed," *Physical Review Letters*, Vol. 65, No. 21, 1990, pp. 2654–2657.
- <sup>5</sup>Klein, H., Schmitz, G., and Woermann, D., "Temperature Propagation in Near-Critical Fluids Prior to and During Phase Separation," *Physical Review A: General Physics*, Vol. 43, No. 8, 1991, pp. 4562, 4563.
- <sup>6</sup>Garrabos, Y., Perrot, F., and Beysens, D., "Heat and Mass Transport in a Hypercompressible Fluid Under Zero Gravity," *Proceedings of the 1st European Symposium "Fluids in Space"*, European Space Agency, Noordwijk, The Netherlands, 1991, pp. 357–384.
- <sup>7</sup>Zappoli, B., Beysens, D., Guenoun, P., Khali, B., Garrabos, Y., and Le Neindre, B., "Anomalies of Heat Transport in Near Critical Fluids Under Weightlessness," *Advances in Space Research*, Vol. 11, No. 7, 1991, pp. 269–276.
- <sup>8</sup>Garrabos, Y., Le Neindre, B., Guenoun, P., Perrot, F., and Beysens, D., "Transport of Heat and Mass in Near-Critical Fluids," *Proceedings of the VIIIth European Symposium on Materials and Fluid Sciences in Microgravity*, European Space Agency, Noordwijk, The Netherlands, 1992, pp. 807–813.
- <sup>9</sup>Guenoun, P., Khali, B., Beysens, D., Garrabos, Y., Kammoun, F., Le Neindre, B., and Zappoli, B., "Thermal Cycle Around the Critical Point of Carbon Dioxide Under Reduced Gravity," *Physical Review E*, Vol. 47, No. 3, 1993, pp. 1531–1540.
- <sup>10</sup>Bonetti, M., Perrot, F., Beysens, D., and Garrabos, Y., "Fast Thermalization in Supercritical Fluids," *Physical Review E*, Vol. 49, No. 6, 1994, pp. 4779–4782.
- <sup>11</sup>Straub, J., Eicher, L., and Haupt, A., "Dynamic Temperature Propagation in a Pure Fluid near its Critical Point Observed Under Microgravity During the German Spacelab Mission D-2," *Physical Review E*, Vol. 51, No. 6, 1995, pp. 5556–5563.
- <sup>12</sup>Kassoy, D. R., "The Response of a Confined Gas to a Thermal Disturbance. I: Slow Transients," *SIAM Journal of Applied Mathematics*, Vol. 36, No. 3, 1979, pp. 624–634.
- <sup>13</sup>Boukari, H., Shaumeyer, J. N., Briggs, M. E., and Gammon, R. W., "Critical Speeding Up in Pure Fluids," *Physical Review*, Vol. 41, No. 4, 1990, pp. 2260–2263.
- <sup>14</sup>Zappoli, B., Bailly, D., Garrabos, Y., Le Neindre, B., Guenoun, P., and Beysens, D., "Anomalous Heat Transport by the Piston Effect in Supercritical Fluids Under Zero Gravity," *Physical Review A: General Physics*, Vol. 41, No. 4, 1990, pp. 2264–2267.
- <sup>15</sup>Onuki, A., and Ferrell, R., "Adiabatic Heating Effect Near the Gas-Liquid Critical Point," *Physica A*, Vol. 164, 1990, pp. 245–264.
- <sup>16</sup>Behringer, R. P., Onuki, A., and Meyer, H., "Thermal Equilibration of Fluids near the Liquid-Vapor Critical Point:  $^3\text{He}$  and  $^3\text{He}$ - $^4\text{He}$  Mixtures," *Journal of Low Temperature Physics*, Vol. 81, No. 1, 1990, pp. 71–102.
- <sup>17</sup>Zappoli, B., "The Response of a Nearly Supercritical Pure Fluid to a Thermal Disturbance," *Physical Review Fluids A*, Vol. 4, May 1992, pp. 1040–1048.
- <sup>18</sup>Djennanaoui, N., Heraudeau, F., Guenoun, P., Beysens, D., and Zappoli, B., "Thermal Transport in a Pure Fluid near the Critical Point," *41st Congress of the International Astronautical Federation*, International Academy of Astronautics, Paris, 1990, pp. 189–193; also *Acta Astronautica*, Vol. 29, No. 3, 1993, pp. 189–193.
- <sup>19</sup>Zappoli, B., Amiroudine, S., Cales, P., and Ouazzani, J., "Numerical Solutions of Thermoacoustic and Buoyancy-Driven Transport in a Near Critical Fluid," *Materials and Fluids Under Low Gravity*, Springer-Verlag, Berlin, 1996, p. 27.
- <sup>20</sup>Hendricks, R. C., Baron, A. K., and Peller, I. C., "GASP—A Computer Code for Calculating the Thermodynamic and Transport Properties for Ten Fluids: Parahydrogen, Helium, Neon, Methane, Nitrogen, Carbon Monoxide, Oxygen, Fluorine, Argon, and Carbon Dioxide," NASA TND-7808, Feb. 1975.
- <sup>21</sup>Emanuel, G., "Introduction to Critical Point Theory with Application to Fluid Mechanics," AIAA Paper 96-2129, June 1996.
- <sup>22</sup>Nwobi, O. C., Long, L. N., and Micci, M. M., "Molecular Dynamics Studies of Properties of Supercritical Fluids," *Journal of Thermophysics and Heat Transfer*, Vol. 12, No. 3, 1998, pp. 322–327.
- <sup>23</sup>Arpaci, V. S., and Larsen, P. S., *Convection Heat Transfer*, Prentice-Hall, Upper Saddle River, NJ, 1984, p. 49.
- <sup>24</sup>Zappoli, B., Carles, P., Amiroudine, S., and Ouazzani, J., "Inversion of Acoustic Waves Reflection Rules in the Near Critical Pure Fluid," *Physics of Fluids*, Vol. 7, No. 9, 1995, pp. 2283–2287.
- <sup>25</sup>Patankar, S. V., *Numerical Heat Transfer and Fluid Flow*, Hemisphere, Washington, DC, 1980.